

RESEARCH LETTER

10.1002/2014GL061869

Key Points:

- Loss cones of energetic and low-energy particles may be significantly different
- The difference results from next order terms of the magnetic moment
- The qualitative and quantitative changes affect energetic particle precipitation

Correspondence to:

J. R. Johnson,
jjr@pppl.gov

Citation:

Porazik, P., J. R. Johnson, I. Kaganovich, and E. Sanchez (2014), Modification of the loss cone for energetic particles, *Geophys. Res. Lett.*, *41*, 8107–8113, doi:10.1002/2014GL061869.

Received 16 SEP 2014

Accepted 4 NOV 2014

Accepted article online 7 NOV 2014

Published online 28 NOV 2014

Modification of the loss cone for energetic particles

Peter Porazik¹, Jay R. Johnson¹, Igor Kaganovich¹, and Ennio Sanchez²

¹Princeton Center for Heliophysics, Plasma Physics Laboratory, Princeton University, Princeton, New Jersey, USA, ²Center for Geospace Sciences, SRI International, Menlo Park, California, USA

Abstract The optimal pitch angle which maximizes the penetration distance, along the magnetic field, of relativistic charged particles injected from the midplane of an axisymmetric field is investigated analytically and numerically. Higher-order terms of the magnetic moment invariant are necessary to correctly determine the mirror point of trapped energetic particles, and therefore the loss cone. The modified loss cone resulting from the inclusion of higher-order terms is no longer entirely defined by the pitch angle but also by the phase angle of the particle at the point of injection. The optimal orientation of the injection has a nonzero component perpendicular to the magnetic field line, and is in the plane tangential to the flux surface. Numerical integration of particle orbits were carried out for a relativistic electron in a dipole field, showing agreement with analytic expressions. The results are relevant to experiments, which are concerned with injection of relativistic beams into the atmosphere from aboard a spacecraft in the magnetosphere.

1. Introduction

Experiments using artificial electron beams of keV energies, injected from Earth-orbiting satellites, have been performed for a number of decades [Winckler, 1980; Neubert and Banks, 1992; Krause *et al.*, 1998]. Advancements in accelerator technology have recently made it possible for spacecraft to carry aboard a compact linear accelerator capable of producing electron beams of relativistic energies. Particle-in-cell simulations applied to MeV-energy electron beams indicate that relativistic beams are considerably more stable than keV-energy beams due to the higher relativistic electron mass, a lower beam density, and a smaller effect from spacecraft charging [Neubert and Gilchrist, 2002, 2004]. The superior stability should allow a larger fraction of the emitted flux to travel longer distances thus opening up the possibility to use the beams as efficient tracers of magnetic field lines in the magnetosphere. In addition to field-line tracing, other possible suggested uses are the excitation of electromagnetic waves, active modification of near-Earth plasma environment, and measurement of the magnetospheric plasma response [Neubert and Gilchrist, 2002; Starodubtsev and Krafft, 2010; Committee on a Decadal Strategy for Solar and Space Physics (Heliophysics) *et al.*, 2013; Delzanno *et al.*, 2013].

Challenges associated with the injection of relativistic beams from an Earth-orbiting satellite into the atmosphere include beam stability, spacecraft charging, and signal detection. A relatively less discussed topic has to do with conditions under which the atmosphere is accessible to energetic particles injected from the magnetosphere, even if other challenges are overcome. Estimates of the adiabatic loss cone suggest that injection along the magnetic field line should guarantee particle precipitation into the atmosphere. However, if the particle energy is large enough, it may be necessary to consider higher-order terms of the magnetic moment adiabatic invariant, and this then implies that the adiabatic loss cone estimates should be modified. The adiabatic loss cone is reviewed in the next section, followed by a discussion on its modifications due to higher-order terms of the magnetic moment. Next, a derivation of more general loss cone angles is described, along with an example using a dipole approximation of the Earth's magnetic field. The results are summarized in the last section.

2. Adiabatic Loss Cone

In a nonuniform magnetic field, charged particles may become trapped. Trapping restricts the motion of the particle to a particular region along the magnetic field line. The size of this region depends on the reflection point of the particle, called the mirror point. At the mirror point the particle has no velocity directed along the field line; that is, all of its energy is in the perpendicular direction. The location of the mirror point

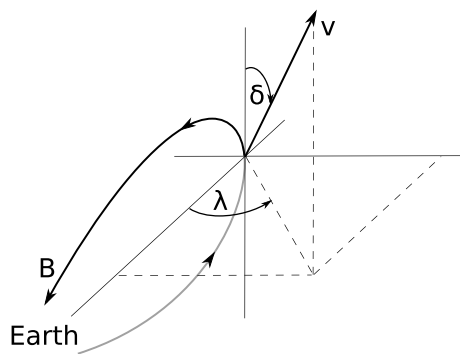


Figure 1. Illustration of the angles δ and λ which define the orientation of the initial velocity vector of a particle initialized at the midplane of an axisymmetric magnetic field, in this case that of the Earth.

is typically estimated using conservation of energy and conservation of magnetic moment $\mu \equiv mv_{\perp}^2/2B(\mathbf{r})$, where m is the mass of the particle, v_{\perp} is its velocity perpendicular to the magnetic field, and $B(\mathbf{r})$ is the magnetic field as well as the assumption that the particle's guiding center remains on the same field line throughout its motion. In terms of the magnetic moment, the kinetic energy of the particle is $E = mv_{\parallel}^2/2 + \mu B(\mathbf{r})$, where v_{\parallel} is the velocity along the magnetic field line. Defining the initial pitch angle in terms of initial velocities as $\tan \delta = v_{\perp}^{\text{init.}}/v_{\parallel}^{\text{init.}}$ [Dungey, 1965], it is then found that δ is related to the magnetic fields at the initial position $B^{\text{init.}}$ and at the mirror point $B^{\text{mirr.}}$ by

$$\sin^2 \delta = \frac{B^{\text{init.}}}{B^{\text{mirr.}}} \tag{1}$$

Larger values of $B^{\text{mirr.}}$ correspond to smaller values of pitch angles δ . The loss cone determines the range of pitch angles, $0 < \delta < \delta_{\text{lc}}$, whose $B^{\text{mirr.}}$ exceeds some predefined value, $B_{\text{lc}}^{\text{mirr.}}$. In the case of the magnetosphere, the predefined value may be the magnetic field at the atmosphere, so that any particles whose pitch angle is smaller than δ_{lc} have mirror points inside the atmosphere and are therefore considered to be lost.

In the case of an ideal dipole field,

$$B = D\sqrt{4 - 3 \cos^2 \phi}/r^3, \tag{2}$$

where D is the dipole moment, r is the radial distance, and ϕ is the angle measured from the equatorial plane toward the z axis. The loss cone is then given by

$$\sin^2 \delta_{\text{lc}} = a^3 \sqrt{\frac{4 - 3 \cos^2 \phi^{\text{init.}}}{4 - 3a \cos^2 \phi^{\text{init.}}}}, \tag{3}$$

where $a \equiv r_{\text{lc}}^{\text{mirr.}}/r^{\text{init.}}$, and the conservation of the magnetic flux $\psi = D \cos^2 \phi/r$ was used. Thus, for a particle injected from the equatorial plane ($\phi^{\text{init.}} = 0$) at a distance of $r^{\text{init.}} = 6.6R_E$, the loss cone into the atmosphere at $r_{\text{lc}}^{\text{mirr.}} = 1R_E$ is $\delta_{\text{lc}} \approx 2.85^\circ$. Note that the boundary which distinguishes trapped from lost particles may be arbitrarily chosen to suit a particular experimental or physical scenario. Here it is chosen to be at the approximate location of the atmosphere.

3. Magnetic Moment Invariant

The loss cone defined in the previous section assumes conservation of the magnetic moment $mv_{\perp}^2/2B(\mathbf{r})$, and based on equation (1), it may be concluded that particles with pitch angle of $\delta = 0$ are always lost. These particles have no initial v_{\perp} , and thus, their magnetic moment is also zero. However, the magnetic moment, as given above, is only the zeroth-order term, $\mu^{(0)}$, of a more general adiabatic invariant corresponding to the cyclotron motion, μ , which is an asymptotic series in the small parameter ρ/L_B [Northrop, 1963]. Here the numerator ρ is the effective Larmor radius, defined by v/Ω_c , where v is the initial velocity of the particle (total, not just v_{\perp}), Ω_c is the cyclotron frequency of the particle $|q||B|/mc$, q is the particle's charge; and m is its relativistic mass, given by $m_0\gamma$, where m_0 is the rest mass of the particle, and $\gamma \equiv 1/\sqrt{1 - v^2/c^2}$. In the case under consideration the electric field is zero, and therefore γ is constant. The denominator, L_B , of the small parameter is the characteristic gradient length scale of the magnetic field $L_B^{-1} = |\nabla \ln B|$. Consequently, even if $\mu^{(0)} = 0$, μ itself is generally finite, corresponding to next order terms of the asymptotic series. Particle reflection therefore occurs even if $\delta = 0$. This effect is especially exaggerated for energetic particles, whose ρ/L_B is more significant.

Although there are a number of systematic methods to derive higher-order components of the magnetic moment μ , the task is in general nontrivial. (General discussion may be found in Northrop [1963] and

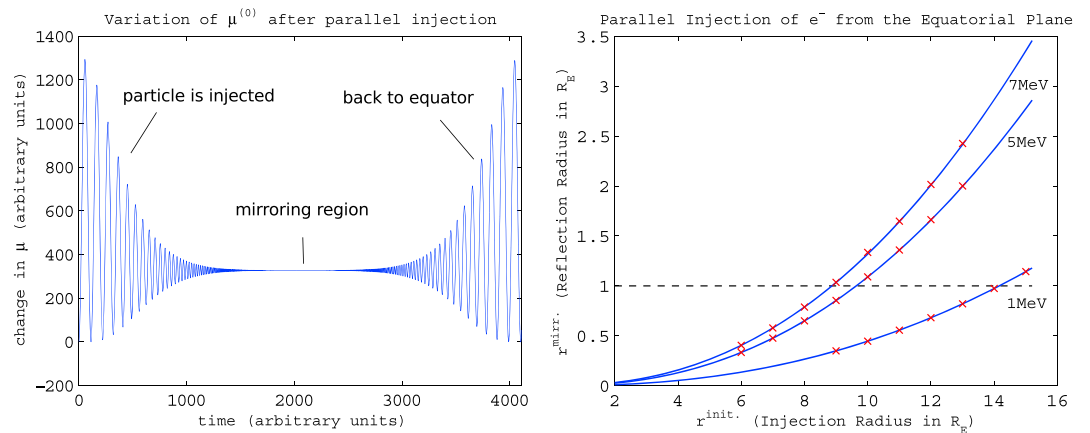


Figure 2. (left) Relative variation of $\mu^{(0)}$ for a 7 MeV electron injected from $10R_E$ at the equatorial plane of a dipolar field with Earth’s dipole moment. (right) The solid lines correspond to mirror points for an electron initialized along the field line from the equatorial plane of a dipole field with Earth’s magnetic moment. The crosses are solutions obtained by numerical integration of particle orbit. The dashed horizontal line at $1R_E$ designates the approximate location of the atmosphere, below which particles are taken to be lost.

Lichtenberg and Lieberman [1992], and some specific methods may be found in Kruskal [1958], Gardner [1959], and Hastie et al. [1967]. Automation of the procedure for arbitrary fields using the Mathematica package VEST (Vector Einstein Summation Tools) [Squire et al., 2014] has recently been described in Burby et al. [2013].) For an axisymmetric field and particle initialization at the midplane, an expression up to and including $O(\epsilon^2)$ has been given in Gardner [1966] as

$$\begin{aligned} \mu &\approx \mu^{(0)} + \epsilon \mu^{(1)} + \epsilon^2 \mu^{(2)} \\ &= \frac{mv_{\perp}^2}{2B} - \epsilon \frac{mcB'}{2B^3} (v^2 + v_{\parallel}^2) v_{\theta} \\ &\quad + \epsilon^2 \frac{m}{2} \left\{ \frac{c^2 B'^2}{B^5} \left[\frac{1}{2} (3v_{\theta}^2 + v_{\parallel}^2) (v^2 + v_{\parallel}^2) + \frac{3}{8} v_{\perp}^4 \right] \right. \\ &\quad - \frac{c^2 B''}{2B^4} \left[v_{\theta}^2 v_{\parallel}^2 + \left(v_{\theta}^2 + \frac{1}{4} v_{\perp}^2 \right) (v^2 + v_{\parallel}^2) \right] \\ &\quad \left. + \frac{c^2 B'}{2rB^4} \left[v_{\theta}^2 v^2 - v_{\perp}^2 v_{\parallel}^2 - \frac{5}{4} v_{\perp}^2 (v^2 + v_{\parallel}^2) + 2v_{\theta}^2 v_{\parallel}^2 \right] \right\}, \end{aligned} \quad (4)$$

where $v_{\theta} = v \sin \delta \sin \lambda$, $v_{\perp} = v \sin \delta$, $v_{\parallel} = v \cos \delta$, $B' = dB/dr$, and angles δ and λ are illustrated in Figure 1, and $\epsilon = m/q$ was introduced as a convenient way to keep track of cyclotron time scales and thus the ordering. The angle δ has the same meaning as the previously defined pitch angle with range $0 \leq \delta \leq \pi$, and the new angle λ describes the azimuthal orientation of the initial velocity of the particle about the field line, with range $0 \leq \lambda \leq 2\pi$. The importance of higher-order terms of the magnetic moment is reflected in the dependence of the particle phase space on angle λ . More specifically, because $\mu^{(0)} = mv_{\perp}^2/2B$ is independent of λ , the loss cone of the previous section is completely determined by the initial pitch angle of the particle, δ . Inclusion of higher-order terms of magnetic moment μ will therefore introduce λ dependence in the loss cone calculation.

The effects of the higher-order terms on the loss cone are especially exaggerated when the particle is initialized with zero pitch angle, $\delta = 0$. Although such a particle has $\mu^{(0)} = 0$ initially, its adiabatically conserved magnetic moment, μ , is approximately $\epsilon^2 \mu^{(2)}$. More specifically, as seen from equation (4) by setting v_{\perp} and v_{θ} to zero, the only surviving term is of $O(\epsilon^2)$ and is proportional to v_{\parallel}^4 .

The variation of $\mu^{(0)}$ for a 7 MeV electron injected from the distance of $10R_E$ at the equatorial plane of a dipolar field with Earth’s magnetic moment ($D = -3.3256 \times 10^4 \text{ nT } R_E^3$) is shown in Figure 2 (left). Due to the relatively weak field at the equatorial plane, the oscillations of $\mu^{(0)}$ are initially large. As the particle moves into the stronger field, it slows down and begins mirroring. At the mirror point, it has no velocity component along the magnetic field line, and therefore, the dominant contribution to μ at this point comes from $\mu^{(0)}$. Since μ is conserved, the value of $\mu^{(0)}$ that the particle thus develops is approximately equal to its initial μ ,

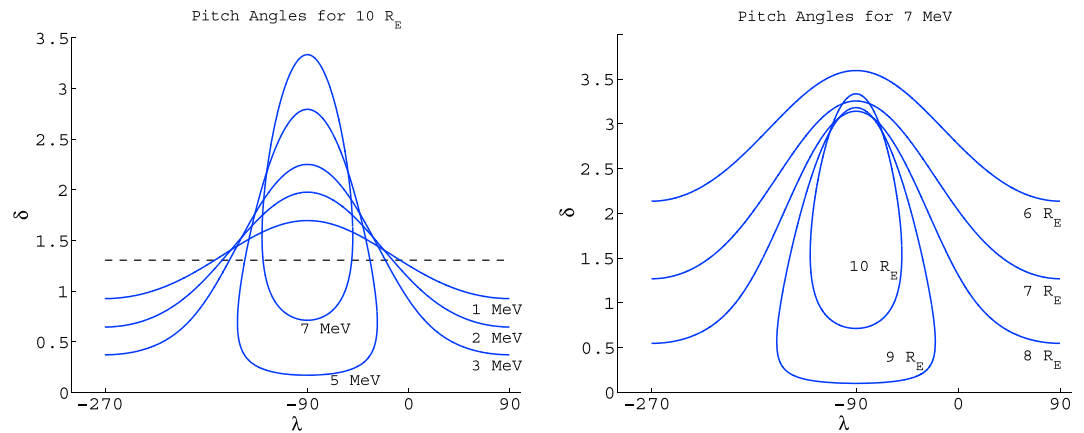


Figure 3. (left) Edges of loss cones for an electron initialized from $10 R_E$ at the equatorial plane of a dipole field for different energies. The black dashed line corresponds to the unmodified loss cone given by equation (3), for the injection from the equatorial plane. (right) Edges of loss cones for a 7 MeV electron initialized from different distances at the equatorial plane of a dipole field.

that is $\epsilon^2 \mu^{(2)}$. The mirror point for a particle injected along the field line from the midplane may therefore be found by equating the initial to the final magnetic moment, i.e., $\mu^{(2)\text{init.}} = \mu^{(0)\text{mirr.}}$, where $\mu^{(0)\text{mirr.}} = mv_{\parallel}^2/2B$, from the conservation of energy.

In the case of the dipole field $\mu^{(2)\text{init.}} = \frac{9mc^2}{2D^3} r^7 v_{\parallel}^4$ from the first ϵ^2 term of equation (4). Then, assuming that the electron's mirror point and its initial point are connected by the same field line, described by the flux function $\psi = D \cos^2 \phi/r$, the mirror point radius, $ar^{\text{init.}}$, for a particle initialized along the field line from the equatorial plane of a dipole field, at radius $r^{\text{init.}}$, is given by the solution of equation

$$9 \left(\frac{\rho_{\parallel}}{r^{\text{init.}}} \right)^2 \sqrt{4 - 3a} = a^3, \tag{5}$$

where $\rho_{\parallel} = v_{\parallel}/\Omega_c^{\text{init.}}$ and $\Omega_c^{\text{init.}} = |q||B^{\text{init.}}|/mc$. The solution is plotted in Figure 2 (right) along with results obtained by numerically integrating electron orbit at various energies. The figure illustrates that, for example, a 7 MeV electron will not reach the atmosphere from the equatorial plane at $10 R_E$ even if its pitch angle is initially zero.

4. Modified Loss Cone

In the previous section, the importance of higher-order terms of the magnetic moment invariant was described, and a method of finding the mirror point for a particle initialized along the field line from the midplane of an axisymmetric magnetic field was given, along with an example for an electron in the ideal dipole field. For a more general initialization, the modified loss cone defining the boundaries between trapped and lost particles in the $\lambda - \delta$ plane has to be determined.

The modified loss cone may be determined by choosing some location beyond which the particles are considered to be lost; combining equations for the conservation of energy and magnetic moment μ ; and assuming that the particle's mirror point and its initial point are on the same field line. The result defines a contour in the $\lambda - \delta$ plane. The contour is the edge of the loss cone, and particles initialized inside this contour are lost. Specifically, the contours are solutions of the equation

$$\begin{aligned} \sin^2 \delta + \Delta \frac{1}{4} \sin \lambda (5 \sin \delta + \sin 3\delta) \\ + \Delta^2 \frac{1}{384} [275 + 68 \cos 2\delta + 41 \cos 4\delta \\ - 4 \cos 2\lambda (43 + \cos 2\delta) \sin^2 \delta] = \frac{a^3}{\sqrt{4 - 3a}}, \end{aligned} \tag{6}$$

where $\Delta \equiv \text{sgn}(-q) \frac{\rho}{L_B} = \text{sgn}(-q) \frac{3v}{r^{\text{init.}} \Omega_c^{\text{init.}}}$.

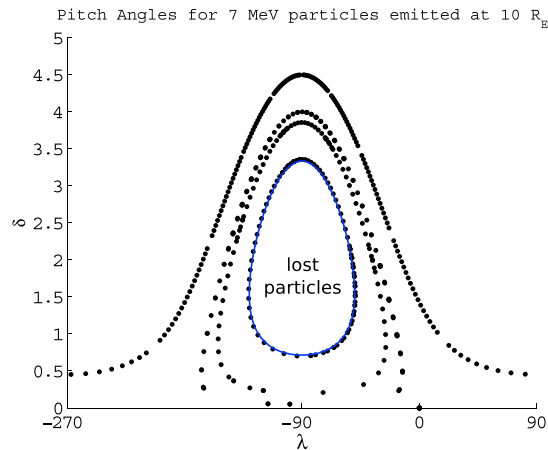


Figure 4. Comparison between numerical integration (dotted lines) of electron orbit for a 7 MeV particle and analytic computation of the loss cone (solid line). Each dot forming a dotted line corresponds to a value of λ and δ at the time of equatorial crossing of a trapped particle. A particle whose initial conditions result in it being trapped will trace out one such line. There are no lines inside the innermost oval, because all particles initialized at these angles were lost.

Results for an electron of different energies initialized from $10 R_E$ at the equatorial plane are shown in Figure 3 (left). The electron is considered to be lost if its mirror point is at the radial distance of $1 R_E$ or less. For comparison, the dashed line shows the loss cone computed based on only the lowest-order term of the magnetic moment, $\mu^{(0)}$. The importance of higher-order terms is most dramatically reflected in the λ dependence of the loss cone. The origin of the λ dependence is mainly the $O(\epsilon)$ term of μ . As the energy of the electron increases, the λ dependence becomes more pronounced, and eventually the loss cone becomes a closed contour with unique boundaries in both angles. The largest range of δ angles is always at $\lambda = -90^\circ$, in the direction of electron drift, tangential to the flux surface (for positive ions, the sign of λ would be positive).

Figure 3 (right) shows the loss cone for a 7 MeV electron initialized in the equatorial plane at different distances. As the distance increases, the loss cone again becomes confined to small region in phase space, with unique boundaries in both angles. The importance of the higher-order terms of the magnetic moment at larger distances can be understood from the consideration of the parameter ρ/L_B , discussed in the previous section. At larger distances, the curvature of the field decreases and therefore L_B increases. But, as the magnetic field becomes weaker, the Larmor radius increases. For the dipole field, the Larmor radius is proportional to r^3 , and L_B is proportional to r ; thus, ρ/L_B increases with distance as r^2 .

The modifications to the loss cone computed by taking into account the higher-order components of the magnetic moment were checked by numerically integrating the electron orbit in the dipole field. The results are shown in Figure 4. Each dot on the plot represents the value of angles λ and δ at the time of equatorial crossing of a trapped particle, i.e., the particle whose mirror point is above $1 R_E$. Multiple crossings thus trace out a line in the $\lambda - \delta$ space. Four such dotted lines are visible in the figure; each line corresponding to different initial conditions of the particle. No lines are shown inside the innermost oval because all particles initialized inside this oval were lost, i.e., had the mirror point below $1 R_E$. The innermost oval thus corresponds to the boundary between trapped and lost particles. The solid line is the loss cone computed analytically, showing agreement with numerical results.

Since the modified loss cone always has the widest range of pitch angles at either $\lambda = -90^\circ$ for electrons or $+90^\circ$ for positive ions, the widest opening of the loss cone may be obtained by setting λ to this value, and solving the following expression for δ

$$\sin^2 \delta - \Delta \frac{1}{4} [5 \sin \delta + \sin 3\delta] + \Delta^2 \frac{1}{384} [275 + 68 \cos 2\delta + 41 \cos 4\delta + 4(43 + \cos 2\delta) \sin^2 \delta] = \frac{a^3}{\sqrt{4 - 3a}}, \quad (7)$$

where Δ for the dipole field is $\frac{\rho}{L_B} = \frac{3v}{r_{\text{init}} \Omega_c^{\text{init}}}$. The solution of this equation gives the upper and lower bounds of the largest range of pitch angles which correspond to lost particles, provided λ is oriented in the direction of particle drift as described above. When $\Delta = 0$, this expression reduces to equation (3), for the

injection from the equatorial plane. Using the fact that δ is typically small, equation (7) may be expanded around $\delta = 0$ to yield

$$\Delta^2 - 2|\Delta|\delta - \frac{1}{4}(3\Delta^2 - 4)\delta^2 = \frac{a^3}{\sqrt{4 - 3a}}. \quad (8)$$

$$(\delta - \Delta)^2 \approx \frac{a^3}{\sqrt{4 - 3a}} \quad (9)$$

$$\delta \approx \Delta \pm \left(\frac{a^3}{\sqrt{4 - 3a}} \right)^{1/2}, \quad (10)$$

where the second equation was obtained by dropping the $\Delta^2\delta^2$ term from equation (8). The two solutions for δ correspond to the upper and lower bound of closed contours in Figure 3. For a 7 MeV particle injected from $10R_E$, the above approximation gives $\delta_{\min.} = 0.72^\circ$, and $\delta_{\max.} = 3.33^\circ$, as verified by corresponding contours in Figure 3.

5. Discussion

When computing the loss cone, caution should be exercised that it is sufficient to use the conservation of $\mu^{(0)}$ as an underlying assumption. For energetic particles, this may not be the case, and to determine whether a particle is lost, it may be necessary to consider the magnetic moment, μ , up to $O(\epsilon^2)$. It is then found that to ensure that a particle is lost to the atmosphere when it is launched from the magnetospheric equator, it is generally neither necessary nor sufficient to initialize the particle with a zero pitch angle, as would be expected from usual loss cone calculations. Rather, the orientation of the initial particle velocity vector should be described in terms of the angle δ , defining the angular deviation of the velocity vector from the magnetic field line; and the angle λ , defining the degree of rotation of the vector about the plane defined locally by the magnetic field line, as illustrated in Figure 1. The modified loss cone has the largest range in δ when the angle λ is such that the perpendicular component of the initial velocity vector points tangentially to the magnetic flux surface and in the direction of the particle drift—for an electron, this is at $\lambda = -90^\circ$, and for a positive ion, it is at 90° . This is determined by the $O(\epsilon)$ term of the magnetic moment, which depends on the sign of the particle's charge. The two panels of Figure 3 show the effect of the higher-order terms on the loss cone, when lost particles are those whose mirror point is lower than $1R_E$. At high enough energies, or at large distances, the loss cone defines a closed contour in the $\lambda - \delta$ space, so that there is not only a maximum pitch angle δ beyond which the particles are trapped but also a minimum. The modified loss cone calculations were carried out for energetic electrons using the dipole approximation of the Earth's magnetic field. In reality, a more realistic field should be used at distances larger than about $5R_E$, when the dipole approximation becomes less valid. Considering that in a realistic magnetospheric field, the curvature in the midnight sector is increased, and in the noon sector, the compression of the flux surfaces creates magnetic cusps off the equatorial plane; it is reasonable to expect that in reality, the modifications to the adiabatic loss cone should be much more dramatic than presented here for a dipole.

The loss cone modification was obtained using the conservation of energy, magnetic moment, and the assumption that the initial and mirror points of the particle are connected by a single field line. For the dipole field, the flux function describing the magnetic field line is $\psi = D \cos^2(\phi)/r$, and it is assumed to have the same value at the mirror as at the initial points. That the flux function is an adiabatic invariant on time scales longer than the drift period is commonly proved using lowest orders of adiabatic invariants μ and the longitudinal invariant, J . For an axisymmetric magnetic field, such as the dipole, the canonical angular momentum in the azimuthal direction is an exact invariant and is related to the flux function ψ by $p_\theta = mrv_\theta + e\psi$, where (r, θ) are the radial and azimuthal coordinates in the cylindrical coordinate system. The change in ψ from its initial value is therefore of order ϵ^2 , which is small enough to yield accurate estimates for the loss cone using only the initial value of the flux function, as seen from the provided examples.

In context of beam injection from space, the above results are most applicable to ideal regimes in which the beam may be assumed to propagate unaltered by its self-fields, spacecraft charging, collisions, etc. However, even when these effects are not negligible, the results provide guidance on how the optimal orientation for beam injection should be chosen to help ensure that the beam precipitates into the

atmosphere. The angular spread of a typical beam is approximately 0.2° . As seen from Figure 3, this is significantly smaller than the modifications to the loss cone resulting from using the more accurate magnetic moment invariant.

Another possible application is in the study of particle precipitation associated with the Earth's radiation belts. Relativistic electrons with energies upward of 10 MeV populate the inner region of the magnetosphere ($3 < L < 7$) during periods of high-speed solar wind and geomagnetic activity [Paulikas and Blake, 1979]. Knowing the characteristics of the loss cone for different energies and locations in the magnetosphere is critical to understanding the contribution of precipitation of particles to the energy budget of the radiation belts.

Acknowledgments

The data for this paper may be obtained by contacting the corresponding author. The authors acknowledge support from NSF grants AGS-1344303, ATM-0902730, and AGS-1203299 and NASA grants NNNH09AM531, NNNH09AK631, and NNNH11AR071. This manuscript was authored by Princeton University under contract DE-AC02-09CH11466 with the U.S. Department of Energy. This work was facilitated by the Max-Planck/Princeton Center for Plasma Physics. The United States Government retains and the publisher, by accepting the article for publication, acknowledges that the United States Government retains a nonexclusive, paid-up, irrevocable, worldwide license to publish or reproduce the published form of this manuscript, or allow others to do so, for United States Government purposes.

Benoit Lavraud thanks Joseph Borovsky for his assistance in evaluating this paper.

References

- Burby, J. W., J. Squire, and H. Qin (2013), Automation of the guiding center expansion, *Phys. Plasmas*, *20*(7), 072105, doi:10.1063/1.4813247.
- Committee on a Decadal Strategy for Solar and Space Physics (Heliophysics), Space Studies Board, Aeronautics and Space Engineering Board, Division on Engineering and Physical Sciences, and National Research Council (2013), *Solar and Space Physics: A Science for a Technological Society*, Natl. Acad. Press, Washington, D. C.
- Delzanno, G. L., E. Camporeale, E. Hogan, J. D. Moulton, J. Borovsky, E. MacDonald, and M. Thomsen (2013), Probing the Earth's magnetosphere with an electron gun, paper presented at 55th Annual Meeting of the APS Division of Plasma Physics, *58*(16), Denver, Colo, 11-15 Nov.
- Dungey, J. (1965), Effects of electromagnetic perturbations on particles trapped in the radiation belts, *Space Sci. Rev.*, *4*, 199–222.
- Gardner, C. S. (1959), Adiabatic invariants of periodic classical systems, *Phys. Rev.*, *115*, 791–794, doi:10.1103/PhysRev.115.791.
- Gardner, C. S. (1966), Magnetic moment to second order for axisymmetric static field, *Phys. Fluids*, *9*, 1997–2000, doi:10.1063/1.1761557.
- Hastie, R., J. Taylor, and F. A. Haas (1967), Adiabatic invariants and the equilibrium of magnetically trapped particles, *Ann. Phys.*, *41*, 302–338.
- Krause, L. H., B. E. Gilchrist, and T. Neubert (1998), Analysis of active space experiments using artificial relativistic electron beams, paper presented at 6th Spacecraft Charging Conference, 139–142, AFRL Science Center, Hanscom AFB, Mass., 2-6 Nov.
- Kruskal, M. D. (1958), The gyration of a charged particle, *Tech. Rep. PM-5-33*, Princeton Univ., Princeton, N. J.
- Lichtenberg, A. J., and M. A. Leiberman (1992), *Regular and Chaotic Dynamics*, Springer, New York.
- Neubert, T., and P. M. Banks (1992), Recent results from studies of electron beam phenomena in space plasmas, *Planet. Space Sci.*, *40*(2–3), 153–183, doi:10.1016/0032-0633(92)90055-S.
- Neubert, T., and B. E. Gilchrist (2002), Particle simulations of relativistic electron beam injection from spacecraft, *J. Geophys. Res.*, *107*(A8), SIA 9-1–SIA 9-10, doi:10.1029/2001JA900102.
- Neubert, T., and B. E. Gilchrist (2004), Relativistic electron beam injection from spacecraft: Performance and applications, *Adv. Space Res.*, *34*, 2409–2412, doi:10.1016/j.asr.2003.08.081.
- Northrop, T. G. (1963), *The Adiabatic Motion of Charged Particles*, John Wiley, New York.
- Paulikas, G. A., and J. B. Blake (1979), Effects of the solar wind on magnetospheric dynamics: Energetic electrons at the synchronous orbit, in *Quantitative Modeling of Magnetospheric Processes*, *Geophys. Monogr. Ser.*, vol. 21, edited by W. P. Olson, pp. 180–202, AGU, Washington, D. C.
- Squire, J., J. Burby, and H. Qin (2014), VEST: Abstract vector calculus simplification in mathematica, *Comput. Phys. Commun.*, *185*, 128–135, doi:10.1016/j.cpc.2013.08.021.
- Starodubtsev, M. V., and C. Krafft (2010), Laboratory modeling of the interaction of electron beams with a magnetoplasma, *Radiophys. Quantum Electron.*, *53*, 401–416, doi:10.1007/s11141-010-9238-4.
- Winckler, J. R. (1980), The application of artificial electron beams to magnetospheric research, *Rev. Geophys. Space Phys.*, *18*, 659–682, doi:10.1029/RG018i003p00659.